

Reducing Solar Heat Gain from Inclined Buildings' Roof by Using Radiant Barrier System

Shikha Ebrahim, and Adel Alshayji*

Department of Mechanical Engineering, College of Engineering and Petroleum, Kuwait University

*Corresponding author: P. O. Box 5969, Safat, 13060, a.alshayji@ku.edu.kw

Abstract: Energy conservation in buildings is one of the most significant areas of study. Many researches were accomplished in this field since it is cost effective method to reduce the energy consumed in buildings. In this study, the effect of applying radiant barrier system (RBS) to the buildings' roof was investigated numerically using COMSOL. The study produced simulated model of natural convection in an inclined rectangular channel open ended with different locations of RB along the channel thickness (S). The upper plate is heated by various uniform constant heat fluxes while the inner surface of the lower plate has a very thin layer with low emissive aluminum foil (RBS). The dimensions of the model are (thickness \times width \times length) 0.05 m \times 0.7 m \times 1.5 m, respectively. This model was used to adjust the location of RB in the air gap between the plates of the channel at a fixed angle 15° and four different uniform heat fluxes: $q_s = 190.5, 285.7, 380.9$ and 472.9 W/m². The objective of this study is to measure the heat flux passing through the lower plate as the location of RB alters. As a result, RB reduces heat gain into the roof by almost 77%. Moreover, Nusselt number (Nu) and Reynolds number (Re) correlations are determined to calculate heat transfer coefficient as a function of Rayleigh number (Ra) and RB location (A).

Keywords: Radiant barrier system (RBS), Natural convection, Inclined roof, Surface-to-surface radiation.

1. Introduction

Free convection plays an important role in many engineering applications and naturally occurring processes [1]. Many researches were accomplished experimentally and numerically [2], [3-12]) to analyze heat transfer in an attic under laminar conditions. Few studies were investigated under a turbulent flow conditions [2], [13-14]). Shimin et al. studied the turbulent airflow and heat transfer in both sealed and vented attic through developing a computational

fluid dynamic (CFD) model using Reynolds-averaged Navier-Stokes (RANS) model [2].

More attention was received to natural ventilation of buildings as a new alternative source of energy saving [1]. Nowadays, radiant barrier system (RBS) has commonly presented in the market to reduce cooling load in buildings. This system is mainly consisted of thin layer covered by low emissive coating that provides the reflective phenomena (e.g. aluminum foil) [1]. There were many studies done to recognize the performance of RBS in the roofs experimentally [15-17]. Recent study was accomplished by C. Escudero to determine the thermal characteristics of RBS using both analytical and experimental methods [18].

In this study the effect of varying RB location along the air gap between the two plates of the channel was investigated as shown in Figure (1). The variation in RB location is expected to enhance the airflow rate in the channel and to reduce the heat gain into the building.

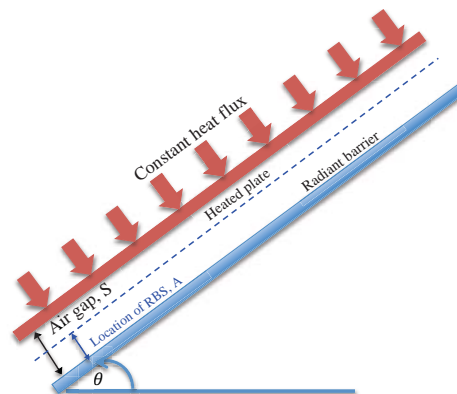


Figure 1. A Schematic of inclined rectangular channel with heated plate and RBS

2. Governing Equations

The non-isothermal flow model was used to simulate the physics of the problem including both heat transfer and fluid flow. The most important governing equations are continuity, momentum, and energy.

$$\nabla \cdot (\rho u) = 0 \quad (1)$$

$$\rho u \cdot \nabla u = -\nabla p + \nabla \cdot \left(\mu (\nabla u + (\nabla u)^T) - \frac{2}{3} \mu (\nabla \cdot u) I \right) + F \quad (2)$$

$$\rho C_p u \nabla T = \nabla \cdot (k \nabla T) \quad (3)$$

Where: ρ : the density (kg/m^3), u : velocity vector (m/s), p : pressure (Pa), μ : dynamic viscosity (Pa.s), F : body force vector (N/m^3), C_p : specific heat capacity at constant pressure (J/kgK), and T : absolute temperature (K).

3. Methods and Approach

This problem considered a heat transfer problem interacted with fluid-flow. Assumptions considered in the simulation:

- Steady state problem.
- Incompressible flow.
- Plates with constant properties.
- Inlet temperature of 26°C .
- Boussinesq approximation is applied.
- Heat is transferred from the lower plate to the room by radiation only.
- The emissivity of radiant barrier is 0.02 and the emissivity of the upper plate is 0.903.

This study considered the effects of RB location on heat flux passing through the lower plate in comparison to a case when no RB was applied. Four different applied heat fluxes at the upper plate, Nusselt number (Nu) and Reynolds number (Re) are calculated for each individual case.

4. Theory

The heat transfer part of the model consists of conduction, convection, and radiation modes. Some non-dimensional parameters were used in defining the physics of heat transfer. Nusselt number was defined as the ratio of convective to conductive heat transfer and it calculated as follows:

$$Nu = \frac{hL}{k} \quad (4)$$

where, h : heat transfer coefficient ($\text{W/m}^2\cdot\text{K}$), L : length of channel (m), and k : fluid thermal conductivity ($\text{W/m}\cdot\text{K}$).

Nusselt number and Reynolds number correlations were proposed to have the following form:

$$Nu = a(Ra \sin 15)^b (A/S)^c \quad (5)$$

$$Re = d(Ra \sin 15)^e (A/S)^f \quad (6)$$

where, a , b , c , d , e , and f are correlation constants.

Heat transfer coefficient is calculated according to this equation:

$$h = \frac{1}{T_1 - T_{bm}} \left(q_s - \frac{\sigma(T_1^4 - T_2^4)}{\frac{1}{\varepsilon_1} - \frac{1}{\varepsilon_2} - 1} \right) \quad (7)$$

where, T_1 : mean surface temperature at heated plate (K), T_{bm} : air bulk mean temperature (K), T_2 : mean surface temperature at radiant barrier (K), σ : Stefan-Boltzmann constant ($\text{W}/(\text{m}^2\cdot\text{K}^4)$), ε_1 : emissivity of heated plate (gypsum board), ε_2 : emissivity of radiant barrier.

Rayleigh number is a dimensionless parameter usually related to buoyancy driven flow (Free convection). It is defined as follows:

$$Ra = \frac{g\beta q_s S^4}{k\nu\alpha} \quad (8)$$

Based on the Boussinesq approximation, the volumetric thermal expansion coefficient is calculated as follows:

$$\beta = \frac{1}{T_{bm}(K)} \quad (9)$$

where, g : acceleration of gravity (m/s^2), ν : air kinematic viscosity (m^2/s), and α : thermal diffusivity of the air (m^2/s).

5. Use of COMSOL

Non-isothermal fluid flow, laminar flow is used in this study. The heat transfer part of the model includes conduction, convection and radiation modes. To involve the radiation in the model, surface-to-surface radiation option is used. First, the depth of the plate is cut to half and a symmetric boundary condition is used to reduce the computational domain. The upper plate is exposed to a constant uniform heat fluxes. The heat is transferred from the lower surface of the upper plate to the channel by convection and radiation. RB helps to reflect most of the received heat and transmit less heat through the

plate. The transmitted heat is discharged to the ambient by radiation (surface-to-ambient radiation). The “open boundary” condition is applied to the inlet and exit of the channel since they are exposed to the atmospheric air. The density of the air varies inside the channel so volume force option is applied to express the effect of body force.

6. Results and Discussion

This section is divided into three parts; the first is a comparison between an experimental work done by Puangsombut, Hirunlabh, and Khedari [19] and our numerical analysis. The second part is a comparison between a channel with and without RB on the lower plate. Finally, the effects of changing RB location through the air gap between the plates.

6.1 Validation

The results have been validated for natural convection in inclined parallel plates by comparing our results using 0.05 m thick channel with those obtained by Puangsombut, Hirunlabh, and Khedari [19]. The outlet velocity, Nusselt number and Reynolds number are compared for several constant heat fluxes. The results fulfill the correlations obtained by Puangsombut, Hirunlabh, and Khedari research shown in equations (9) and (10) and Figures (2) and (3).

$$Nu = 0.5887(Ra \sin 15)^{0.2079} (S/L)^{0.0231} \quad (10)$$

$$Re = 29.207(Ra \sin 15)^{0.1838} (S/L)^{-0.3494} \quad (11)$$

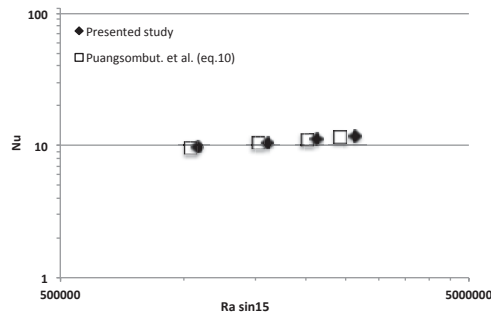


Figure 2. Correlations of Nu and Ra sin 15 at various heat fluxes

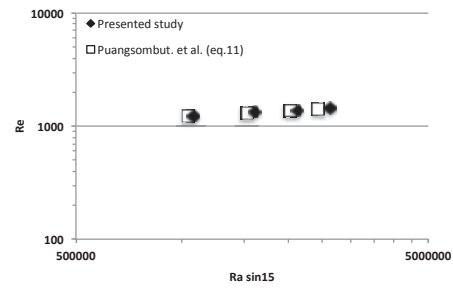


Figure 3. Correlations of Re and Ra sin 15 at various heat fluxes

6.2 Base Case

The purpose of this part of the study is to compare the effects of RB in blocking heat passes the lower plate. Figure (4) shows the heat flux passes through the channel and rejected to the ambient in two cases. The passed Heat fluxes increase as the applied heat fluxes on the upper plate increase. Moreover, heat fluxes pass through the channel is higher in the case of no RB.

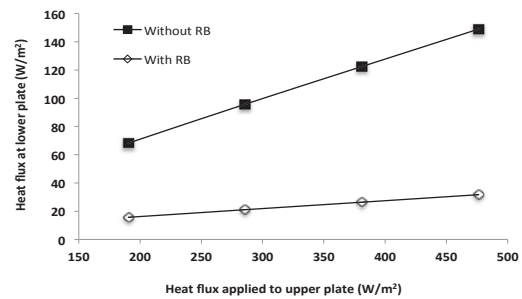


Figure 4. Heat flux passed through the channel for different heat fluxes applied on the upper plate

Figure (5) shows that the velocity is higher when the channel equipped with RB, that’s due to the reflected heat into the channel that enhances the natural convection in the channel.

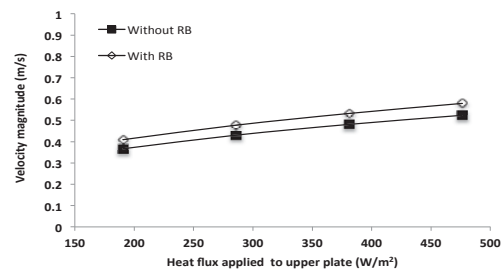


Figure 5. Velocity magnitude at exit of the channel for different heat fluxes applied on the upper plate

The temperature profile of the upper plate is indicated in Figure (6). The temperature increases along the length of the channel as a result of heat accumulation. The temperature of the upper plate is higher when RB is applied. The difference is almost constant between the two curves (around 15°C).

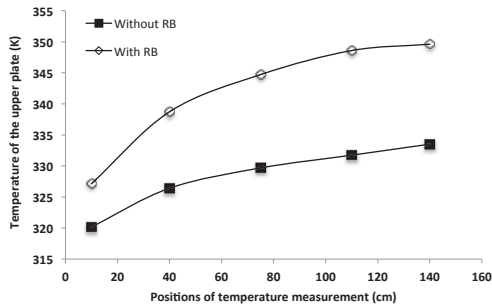


Figure 6. Upper plate temperature distributions along the channels' length for heat flux of 190.5 W/m²

6.3 Varying the location of RB

In this section, the location of RB is varied. It is located at different positions $A = 0.2S, 0.4S, 0.6S,$ and $0.8S$ m.

It is obvious that, as the gap between the RB layer and the upper plate decreases, the temperature of the upper plate increases because the air can't carry more heat as it flows as shown in Figure (7). This figure represents the temperature distributions for a heat flux of 190.5 W/m².

When RB is located at $A = 0.8S$ m, the temperature is increased dramatically because of the narrow channel.

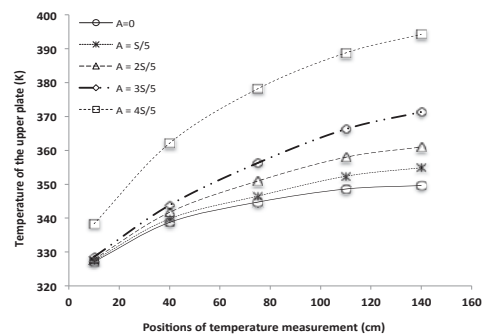


Figure 7. Upper plate temperature distributions along the channels' length for heat flux 190.5 W/m²

The heat flux passes through the lower plate is shown in Figure (8). Compared to the standard case ($A = 0$), implementing RB close to one of

the plates enhances the heat passes through the channel due to low velocity and low convection heat transfer coefficient through the narrow channel. Implementing the RB in the middle of the channel reduces the heat passes through the channel.

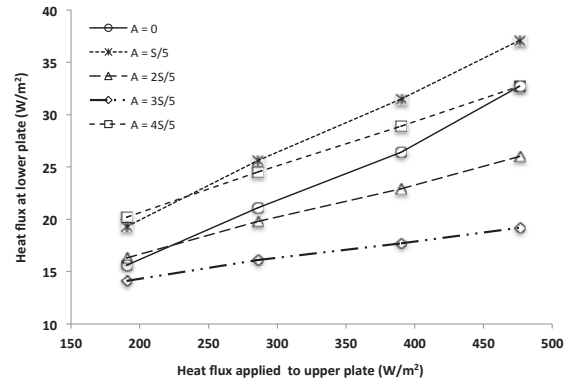


Figure 8. Heat flux pass through the channel for different applied heat fluxes on the upper plate

6.4 Nu and Re correlations

The results obtained are based on fixed inclined angle 15°, five locations of RB, and four constant uniform heat fluxes. Least square method is used to investigate the constants found in equations (5) and (6).

Figure (9) shows the increase in Nu as the heat flux increases when RB is placed on the lower plate. Figure (10) indicates the reduction in Nu values as the location of various RB locations. Table (1) shows a summary of individual correlation.

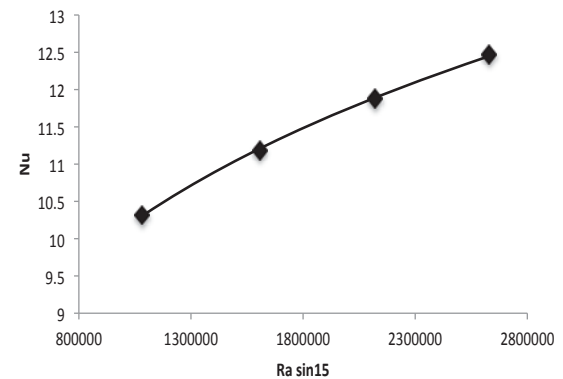


Figure 9. Nu versus Ra sin 15 with RB at the surface of the lower plate

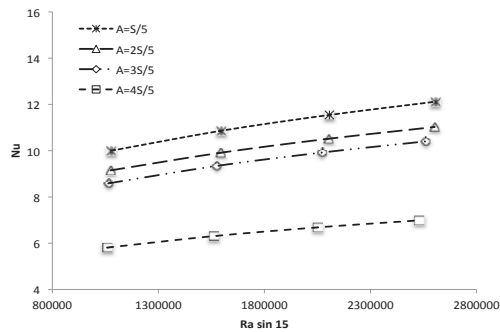


Figure 10. Nu versus Ra sin 15 for different RB locations

Table 1. Summary of Nu correlations for different RB locations

RB Location, cm	Correlation
0	$Nu = 0.5354(Ra \sin 15)^{0.2128}$
S/5	$Nu = 0.4888(Ra \sin 15)^{0.2172}$
2S/5	$Nu = 0.491(Ra \sin 15)^{0.2182}$
3S/5	$Nu = 0.4156(Ra \sin 15)^{0.2182}$
4S/5	$Nu = 0.3073(Ra \sin 15)^{0.2119}$

Similar procedures were done to find a formula of Re for various location of RB along the air gap. Figure (11) shows the increase in Re as the heat flux increases as the heat flux increases when RB is placed on the lower plate. Results are obtained for Re shown in Figure (12) for various RB location. Re correlations are shown in Table (2).

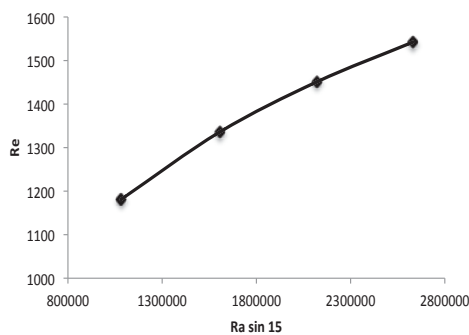


Figure 11. Re versus Ra sin 15 with RB at the surface of the lower plate

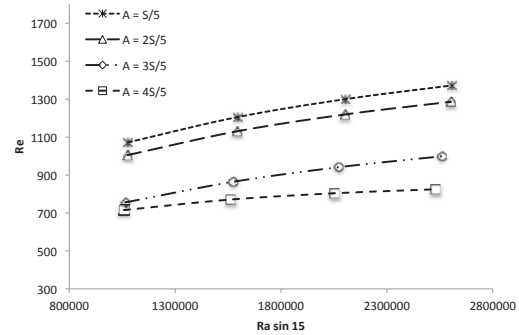


Figure 12. Re versus Ra sin 15 for different RB locations

Table 2. Summary of Re correlations for different RB locations

RB Location, cm	Correlation
0	$Re = 18.078(Ra \sin 15)^{0.3009}$
S/5	$Re = 22.072(Ra \sin 15)^{0.2789}$
2S/5	$Re = 20.644(Ra \sin 15)^{0.28}$
3S/5	$Re = 9.0498(Ra \sin 15)^{0.3191}$
4S/5	$Re = 73.288(Ra \sin 15)^{0.1646}$

Correlations were found to calculate Nu and Re for $A = 0.2S, 0.4S, 0.6S$ and $0.8S$ as shown:

$$Nu = 1.3968(Ra \sin 15)^{0.1156} (A/S)^{-0.2803} \quad (12)$$

$$Re = 15.953(Ra \sin 15)^{0.273} (A/S)^{-0.3068} \quad (13)$$

Figure (13) represents the correlation of Nu versus Ra sin 15 for different RB locations. It was found that Nu decreases as Ra increases. The achieved correlation are valid in the range of $1 \times 10^6 < Ra \sin 15 < 2.5 \times 10^6$ and $6 < Nu < 12$. Figure (14) shows the correlation of Re versus Ra sin 15 for different RB locations. The plot illustrates that Re slightly decreases as Ra increases. The data are achieved for the range $1 \times 10^6 < Ra \sin 15 < 2.5 \times 10^6$ and $700 < Re < 1300$.

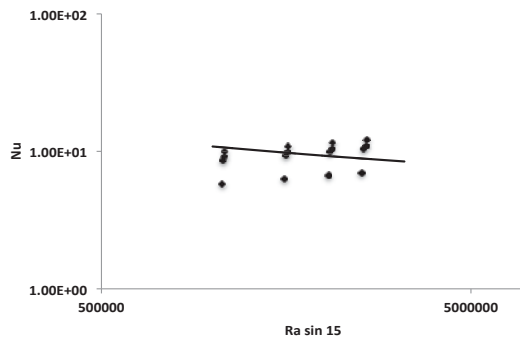


Figure 13. Correlation of Nu and Ra sin 15 for various RB locations

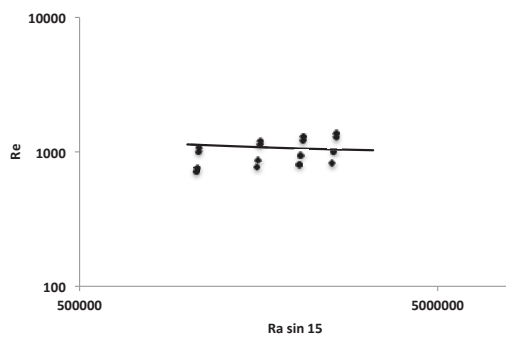


Figure 14. Correlation of Re and Ra sin 15 for various RB locations

7. Conclusions

Numerical study of free convection in an inclined plates heated from the top plate with RB on its lower plate was modeled using COMSOL Multiphysics to evaluate the heat flux passes through the channel.

A validated model was compared to an experimental work done previously. Heat flux passed through channel was compared between a roof equipped with RB and a gypsum board roof. It was found that RB blocked 77% of the heat passes through the channel in gypsum board roof.

The effects of altering the location of RB along the air gap between the plates were studied. Locating RB in the middle of the channel provided a maximum reduction in heat flux passes through the channel. When heat flux of 190.5 W/m^2 is applied to the top plate, 24% reduction in the heat passes is achieved while applying heat flux of 472.6 W/m^2 , 44% reduction in the heat passes is achieved compared to standard case when RB was located on the lower surface.

8. References

1. W. Puangsombut, J. Hirunlabh, J. Khedari, B. Zeghamati, M. M. Win, Enhancement of natural ventilation rate and attic heat gain reduction of roof solar collector using radiant barrier, *Building and Environment*, **42**, (2007), 2218-2226.
2. Shimin Wang, Zhigang Shen, Linxia Gu, Numerical Simulation of buoyancy-driven turbulent ventilation in attic space under winter conditions, *Energy and Building*, **47**, (2012), 360-368.
3. R.D.Flack,C.L.Witt,Velocity measurements in natural convection airflows using a laser velocimeter, *ASME Journal of Heat Transfer* **101** (1979) 256–260.
4. R.D.Flack,The experimental measurement of natural convection heat transfer in triangular enclosures heated or cooled from below, *ASME Journal of Heat Transfer* **102** (1980) 770–772.
5. D. Poulidakos, A. Bejan, Natural convection experiments in a triangular enclosure, *ASME Journal of Heat Transfer* **105** (1983) 652–655.
6. G.A. Holtzman, R.W. Hill, K.S. Ball, Laminar natural convection in isosceles triangular enclosures heated from below and symmetrically cooled from above, *ASME Journal of Heat Transfer* **122** (2000) 485–491.
7. H. Asan, L. Namlı, Laminar natural convection in a pitched roof of triangular cross-section: summer day boundary conditions, *Energy and Buildings* **33** (2000) 69–73.
8. E.H. Ridouane, A. Campo, M. McGarry, Numerical computation of buoyant airflows confined to attic spaces under opposing hot and cold wall conditions, *International Journal of Thermal Sciences* **44** (2005) 944–952
9. C. Lei, S.W. Armfield, J.C. Patterson, Unsteady natural convection in a water-filled isosceles triangular enclosure heated from below, *International Journal of Heat and Mass Transfer* **51** (2008) 2637–2650.
10. E.F. Kent, Numerical analysis of laminar natural convection in isosceles triangular enclosures, Proceedings of the Institution of Mechanical Engineers, Part C, *Journal of Mechanical Engineering Science* **223** (2009) 1157–1169
11. S.C. Saha, J.C. Patterson, C. Lei, Natural convection and heat transfer in attics subject to periodic thermal forcing, *International Journal of*

Thermal Sciences **49** (2010) 1899–1910.

12. S.C.Saha, Unsteady natural convection in a triangular enclosure under isothermal heating, *Energy and Buildings* **43** (2011) 695–703.

13. E.H. Ridouane, A. Campo, M. Hasnaoui, Turbulent natural convection in an air-filled isosceles triangular enclosure, *International Journal of Heat and Fluid Flow* **27** (2006) 476–489.

14. S.O. Talabi, V.O.S. Olunloyo, O.M. Kamiyo, M.W. Collins, T.G. Karayiannis, Flow field and Reynolds stress distribution in low turbulence natural convection in a triangular cavity, in: K. Hanjalic, Y. Nagano, S. Jakirlic (Eds.), *Proc. Fifth International Symposium on Turbulence, Heat and Mass Transfer, Dubrovnik, Croatia, 2006*, pp. 511–514.

15. C. Michels, R. Lamberts, S. Güths, Evaluation of heat flux reduction provided by the use of radiant barriers in clay tile roofs, *Energy and Buildings* **40** (4) (2008) 445–451.

16. S. Roels, M. Deurinck, The effect of a reflective underlay on the global thermal behaviour of pitched roofs, *Building and Environment* **46** (2011) 134–143.

17. M. Medina, On the performance of radiant barrier in combination with different attic insulation levels, *Energy and Buildings* **33** (1) (2000) 31–40.

18. C. Escudero, K. Martin, A. Erkoreka, I. Flores, J. M. Sala, Experimental thermal characterization of radiant barriers for building insulation, *Energy and buildings*, **59**, (2013) 62–72

19. W. Puangsombut, J. Hirunlabh, J. Khedari, An experimental study of free convection in an inclined rectangular channel using radiant barrier, *experimental heat transfer*, **20**(2), (2007), 171–184